Electronic Supplementary Information: Escape dynamics of a self-propelled nanorod from circular confinement with narrow openings

Praveen Kumar and Rajarshi Chakrabarti*

Department of Chemistry,

Indian Institute of Technology Bombay, Mumbai 400076, India

E-mail: rajarshi@chem.iitb.ac.in

The method and parameter validation is carried out for a nanorod in free space. The translational $\left(\left\langle\overline{\Delta r_c^2(\tau)}\right\rangle\right)$ mean square displacement is calculated. From the plot (Fig. S1) for $\mathrm{Pe} = 0$, we have computed the thermal translational diffusion coefficient, $D_T = 1.87\times10^{-5}$ and friction coefficient, $\gamma = 5.33 \times 10^4$.

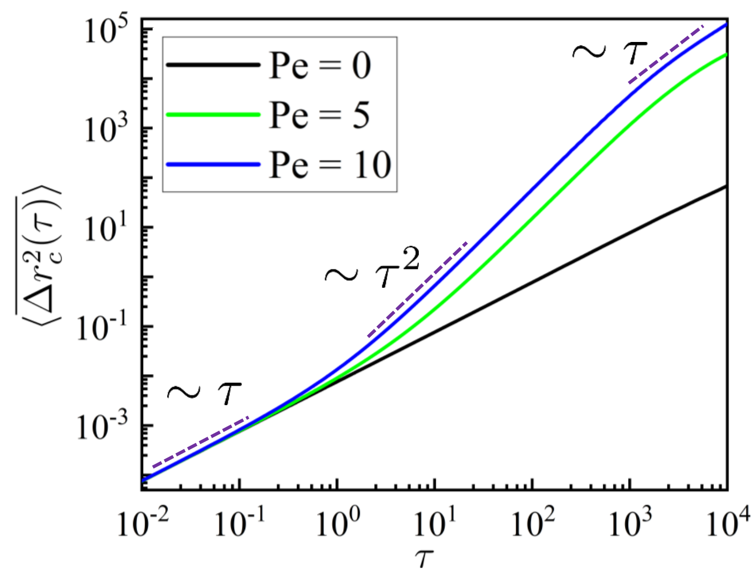

Fig. S1. Log-log plot of $\left\langle\overline{\Delta r_c^2(\tau)}\right\rangle$ for the self-propelled nanorod at different Pe.

For the passive case ($\mathrm{Pe} = 0$), $\left\langle\overline{\Delta r_c^2(\tau)}\right\rangle$ is always diffusive $\left(\left\langle\overline{\Delta r_c^2(\tau)}\right\rangle \sim \tau\right)$ with the diffusion coefficient D_T. In case of the self-propelled nanorod, $\left\langle\overline{\Delta r_c^2(\tau)}\right\rangle$ exhibits three distinct regions: diffusive at short time, superdiffusive region at the intermediate time which scales as $\left\langle\overline{\Delta r_c^2(\tau)}\right\rangle \sim \tau^2$. At longer time, $\left\langle\overline{\Delta r_c^2(\tau)}\right\rangle$ becomes linear in time with an enhanced diffusion coefficient.

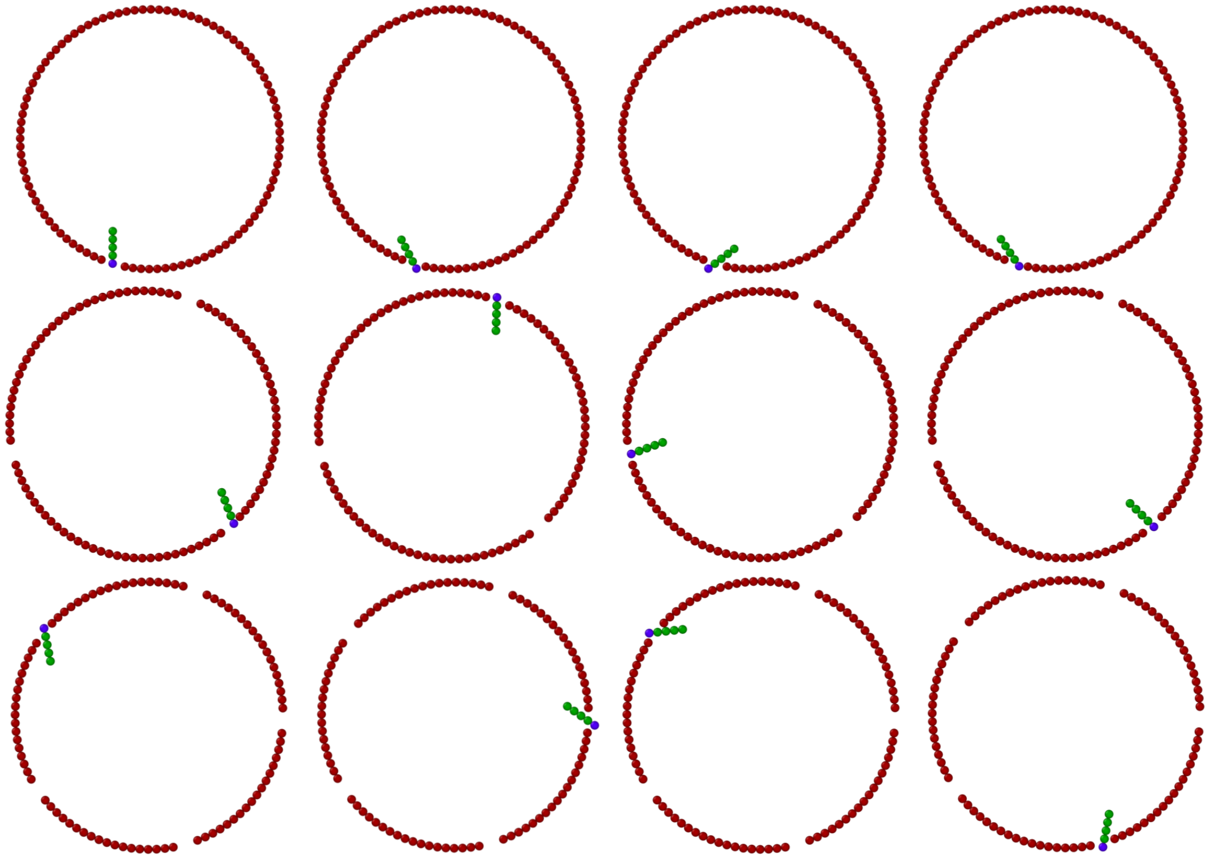

Fig. S2. Here are some snapshots from the simulations where the nanorod successfully escapes through the narrow opening(s) with different orientations.

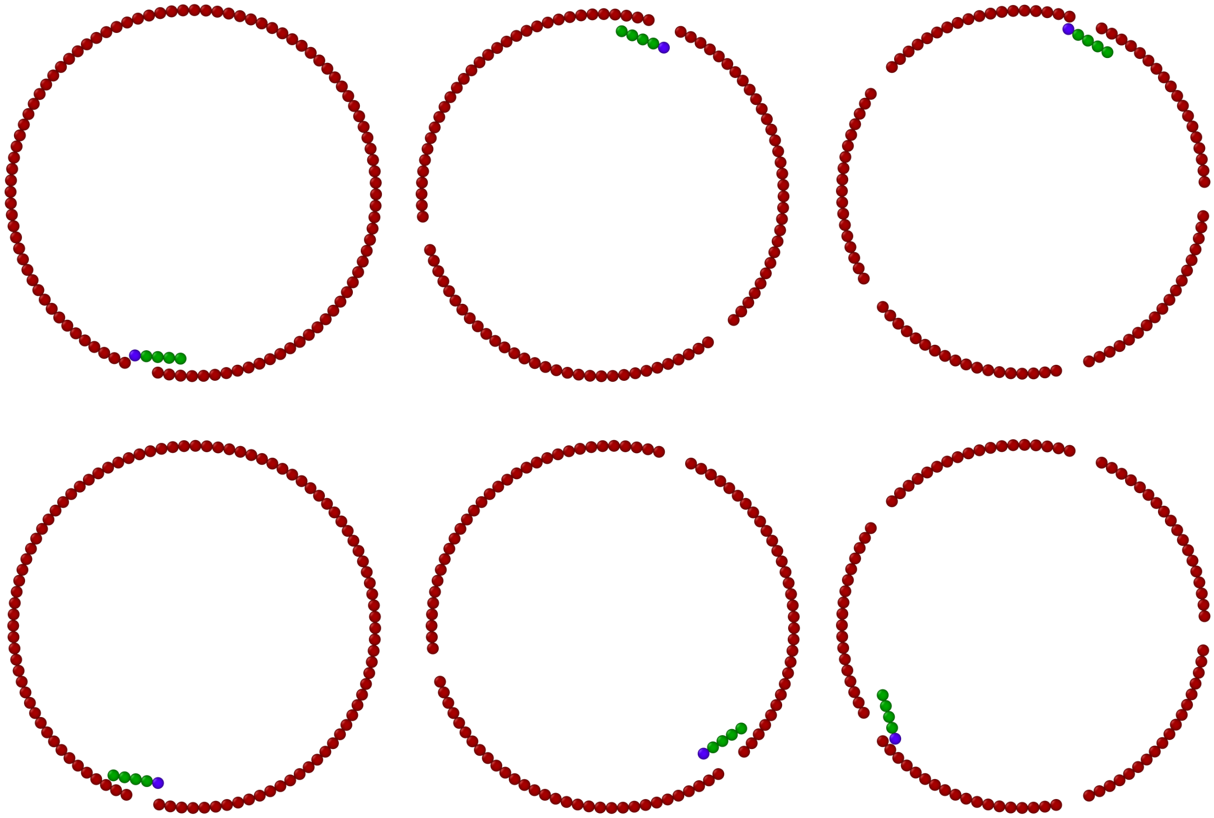

Fig. S3. Here are some snapshots from the simulations depicting instances where the nanorod is unable to escape through the narrow opening(s) due to its improper orientation as it remains nearly parallel to the wall.

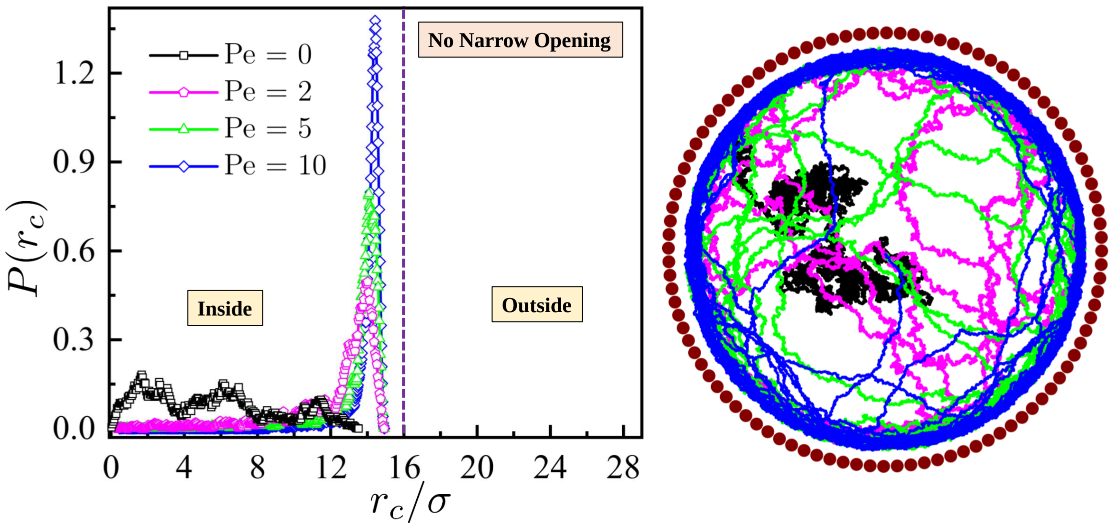

Fig. S4. The radial probability distributions $P(r_c)$ of the nanorod for the confinement without opening, $n_o = 0$ (left) and the corresponding COM trajectories (right) for different Pe.

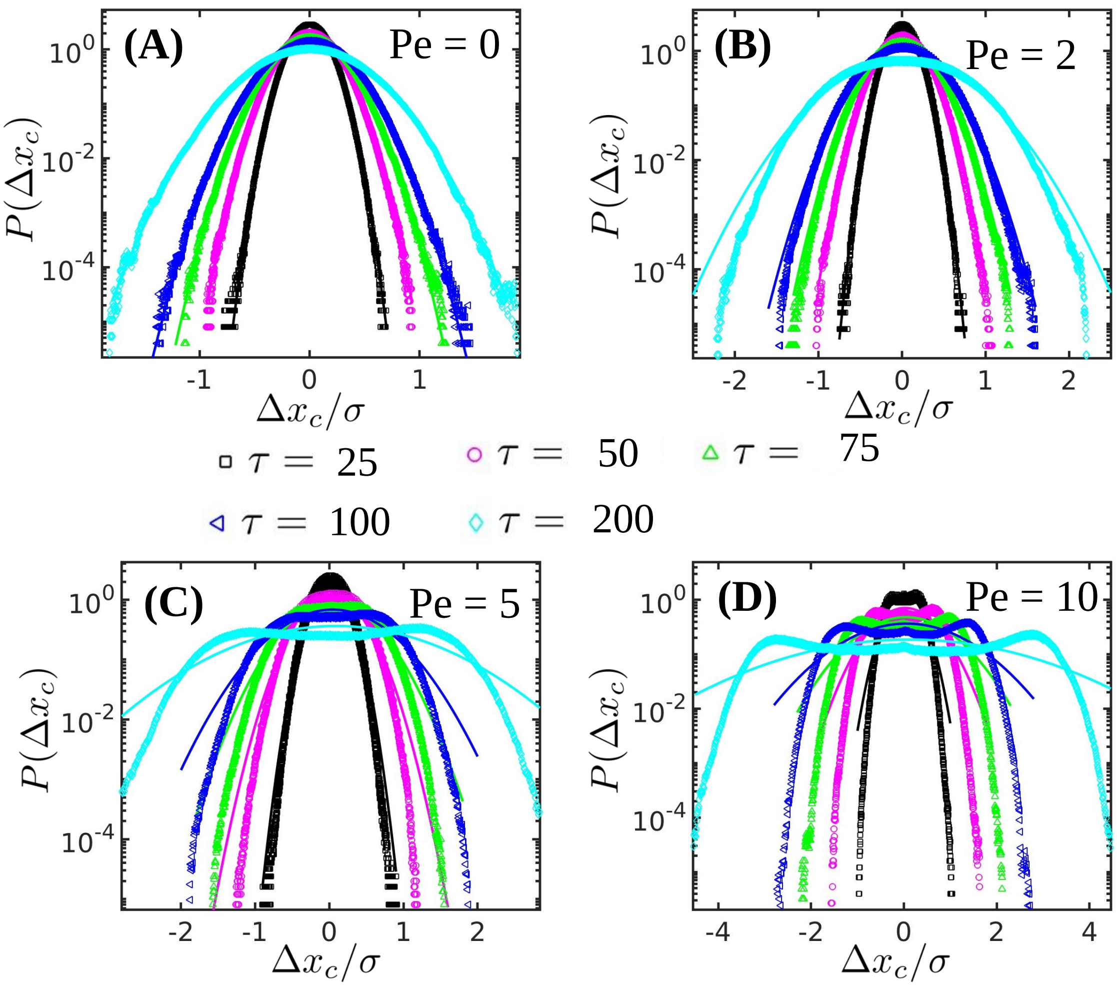

Fig. S5. Plots (A)-(D) represent displacement distribution functions $P(\Delta x_c)$ of a nanorod at different lag times $\tau = 25, 50, 75, 100, 200$ for the confinement with three narrow openings. Solid lines represent the Gaussian fittings.

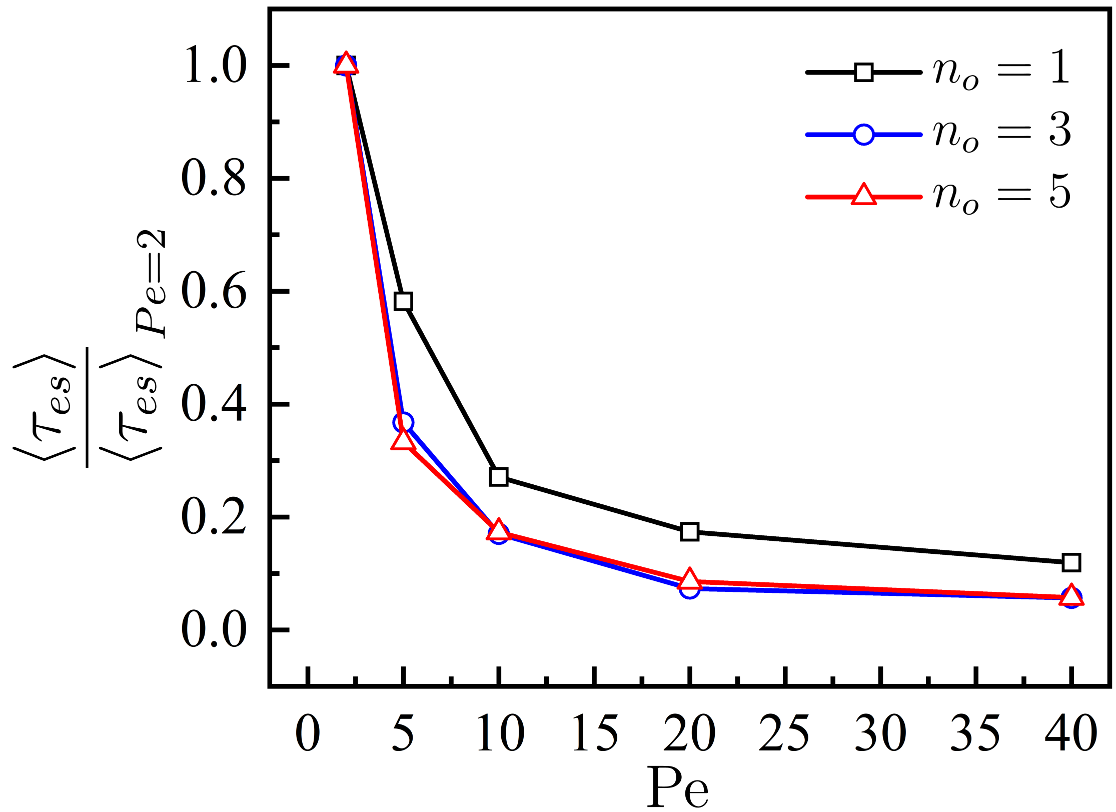

Fig. S6. Plot of $\frac{\langle\tau_{es}\rangle}{\langle\tau_{es}\rangle_{Pe=2}}$ *versus* Pe.

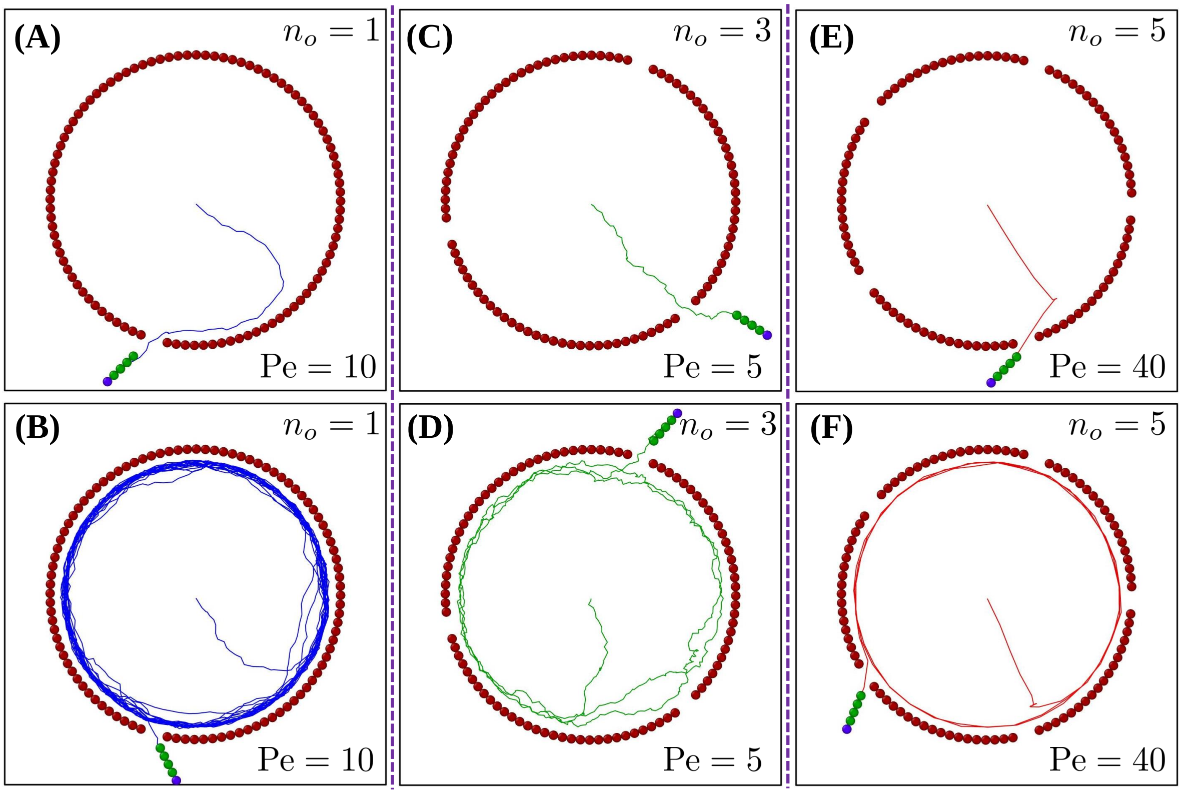

Fig. S7. The COM trajectories of the nanorod in (A) short time escape trajectory, (B) long time escape trajectory at Pe = 10 for a single opening case, (C) short time escape trajectory, (D) long time escape trajectory at Pe = 5 for three openings case, (E) short time escape trajectory, and (F) long time escape trajectory at Pe = 40 for five openings case

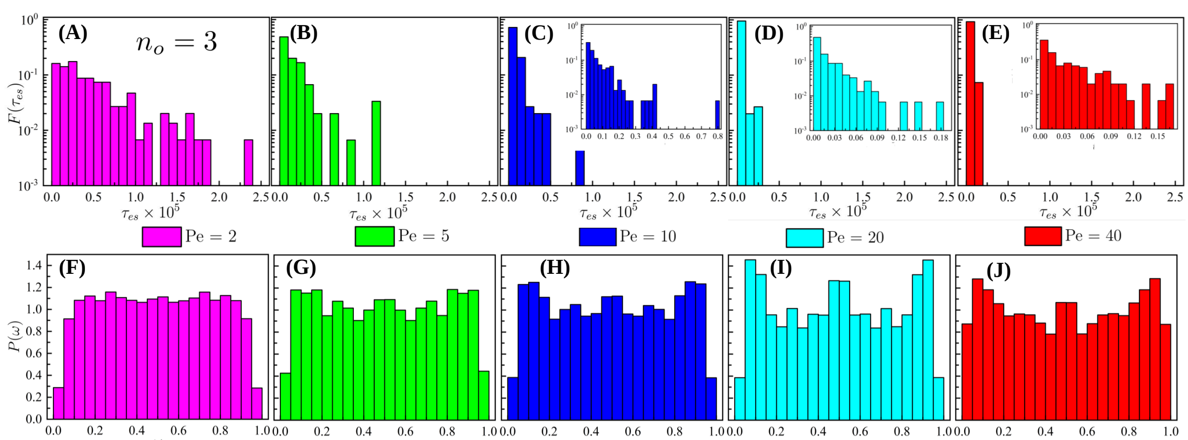

Fig. S8. Plots of the first escape times distributions $F(\tau_{es})$ and corresponding uniformity index distributions $P(\omega)$ of self-driven nanorod are shown in (A-E) and (F-J), respectively, at Pe = $2, 5, 10, 20, 40$, for confinement with three openings.

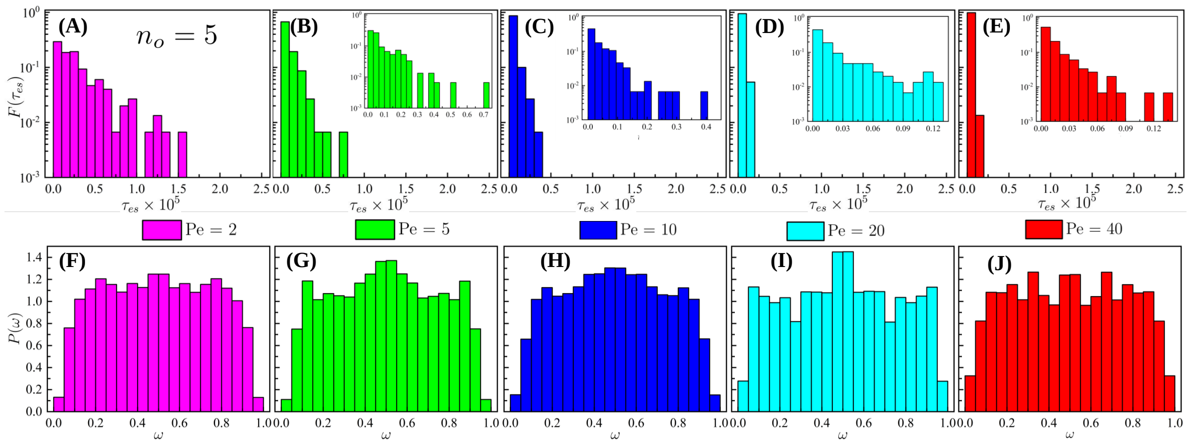

Fig. S9. Plots of the first escape times distributions $F(\tau_{es})$ and corresponding uniformity index distributions $P(\omega)$ of self-driven nanorod are shown in (A-E) and (F-J), respectively, at Pe $= 2, 5, 10, 20, 40$, for confinement with five openings.

Movies

Movie_S1: Brownian dynamics simulation of the passive (Pe = 0) nanorod for the confinement with a single narrow opening ($n_o = 1$).

Movie_S2: Brownian dynamics simulation of the passive (Pe = 0) nanorod for the confinement with three narrow openings ($n_o = 3$).

Movie_S3: Brownian dynamics simulation of the passive (Pe = 0) nanorod for the confinement with five narrow openings ($n_o = 5$).

Movie_S4: Brownian dynamics simulation of the active (Pe = 5) nanorod for the confinement with a single narrow opening ($n_o = 1$).

Movie_S5: Brownian dynamics simulation of the active (Pe = 5) nanorod for the confinement with three narrow openings ($n_o = 3$).

Movie_S6: Brownian dynamics simulation of the active (Pe = 5) nanorod for the confinement with five narrow openings ($n_o = 5$).

Movie_S7: Brownian dynamics simulation of the active (Pe = 20) nanorod for the confinement with a single narrow opening ($n_o = 1$).

Movie_S8: Brownian dynamics simulation of the active (Pe = 20) nanorod for the confinement with three narrow openings ($n_o = 3$).

Movie_S9: Brownian dynamics simulation of the active (Pe = 20) nanorod for the confinement with five narrow openings ($n_o = 5$).

Movie_S10: Brownian dynamics simulation of the active (Pe = 10) nanorod for the confinement with a single narrow opening ($n_o = 1$). Here, the active nanorod quickly moves toward the boundary from the center, finds a small pore, and escapes through it.

Movie_S11: Brownian dynamics simulation of the active (Pe = 10) nanorod for the confinement with a single narrow opening ($n_o = 1$). The active nanorod moves along the boundary repeatedly for a long time.

Movie_S12: Brownian dynamics simulation of the active (Pe = 5) nanorod for the confinement with three narrow openings ($n_o = 3$). Here, the nanorod has a small trajectory.

Movie_S13: Brownian dynamics simulation of the active (Pe = 5) nanorod for the confinement with three narrow openings ($n_o = 3$). Here, the active nanorod moves along the boundary repeatedly for a long time, it has a long circular trajectory.

Movie_S14: Brownian dynamics simulation of the active (Pe = 40) nanorod for the confinement with five narrow openings ($n_o = 5$). Here, the active nanorod quickly escapes through a narrow opening.

Movie_S15: Brownian dynamics simulation of the active (Pe = 40) nanorod for the confinement with five narrow openings ($n_o = 5$). The active nanorod moves along the boundary repeatedly for a long time to escape from the confinement.